



Available online at <http://scik.org>

J. Math. Comput. Sci. 10 (2020), No. 4, 980-1003

<https://doi.org/10.28919/jmcs/4527>

ISSN: 1927-5307

HETEROGENEOUS TRAFFIC FLOW MODELING USING AN EXTENDED PAYNE MODEL WITH STOCHASTIC SOURCE TERM

N'GOLO KONATE^{1,2,*}, DAVID MWANGI THEURI^{1,2}, JOHANA K. SIGEY²

¹Department of Computational Mathematics, Pan African University Institute for Basic Sciences, Technology and Innovation (PAUSTI), P.O. Box 62000-00200, Nairobi, Kenya

²Department of Pure and Applied Mathematics Department, JKUAT P.O. Box 62000-00200, Nairobi, Kenya

Copyright © 2020 the author(s). This is an open access article distributed under the Creative Commons Attribution License, which permits unrestricted use, distribution, and reproduction in any medium, provided the original work is properly cited.

Abstract. In this paper, we are extending Payne model with stochastic source term. The new model differs from that of Payne's in such a way that the traffic pressure and hysteresis are formulate with driver decision. The traditional traffic pressure and hysteresis depend respectively on the traffic density and drivers decision (aggressive-timid, acceleration-deceleration). Our traffic is on an inclined road. In the context of a developing country where the traffic is very heterogeneous and there is a lack of discipline on the highway, the new traffic pressure must take care of the heterogeneity of the traffic. The road traffic hysteresis must take care of the dispersion of the vehicle on the highway. Moreover, the anticipation term is a multi-valued function depending on the vehicle class. The numerical solution of the problem was obtained using a wave analysis. The new model is a hyperbolic one in which the traffic information travels faster than the traffic and the wave propagate downstream leading to a jam formation.

Keywords: traffic flow; stochastic traffic pressure; multivalued anticipation term.

2010 AMS Subject Classification: 60K30.

*Corresponding author

E-mail address: ingngolo@gmail.com

Received February 18, 2020

1. INTRODUCTION

The complexity of traffic nowadays yielded to the irrelevance of the past models. Indeed many parameters such as the road structure, the traffic heterogeneity, the hysteresis have changed the traffic flow modeling. But modeling the heterogeneity of traffic raises some challenges: capture the difference of vehicle in the flow, couple this with driver's behaviors and take consideration of the road structure itself. [1] proposed a non-lane based lattice model through lane separation. The numerical computations and simulation proved that the lane separation enhances the traffic condition. But in this work, the traffic was considered as homogeneous. [2] introduces a new definition of area occupancy to take consideration of the heterogeneity of traffic. His idea of area occupancy is based on the definition of occupancy in [3]. But his area occupancy is limited by the non-consideration of vehicle length in the flow of traffic. Indeed the driver behavior changes in front of a vehicle of different lengths and sizes. Then, the area occupancy impacts the random behavior of drivers. The emergence of high order model such as the one of Payne had corrected the inconsistency of LWR model but had revealed some inconsistency such as its stability in a linear approximation of the stationary solution to smaller perturbation of the traffic result on the formation of a phantom jam or stop and go waves. Thus The traffic pressure was used to correct this inconsistency. Basically The traffic pressure is the way the traffic reduces the speed of a driver. It is proportional to the variance in the traffic speed distribution and is analogous to the gas pressure used in the modeling of gas dynamics. The first traffic pressure was the one in [4] where it was expressed as the product of flow rate and density-dependent speed variance. However, the Phillips traffic pressure was not numerically robust.

The hysteresis is a property of a system to deviate from its original form because of exogenous factors. It's is one of the main parts of traffic oscillation. It can be observed that many of the data points collected are not on the fundamental diagram. Some researchers have explained this phenomenon by stochastic fluctuations but most of the research undertook was deterministic. The impact of traffic hysteresis due to drivers behaviors has received little attention. Among them, the TCI model([6] & [5]) are well known for their capability to explain driver's decision using two concepts: Task Demand and Driver Capability. In his conclusion [7] states that rather

than describes traffic behavior in terms of accelerations and decelerations, like what has been done by many researchers, aggressive and timid behavior exhibit better hysteresis feature as conjectured by [8]. Thus traffic hysteresis has at least two branches in which the dispersion is high in the second part of the diagram. But their relative positions in the fundamental diagram depend on driver behavior. It can be noticed that although hysteresis has been widely studied its scatter properties are still not well formulated.

Considering the criticism made by [9] whereby some macroscopic models for vehicular traffic encounter difficulties showing nonphysical effects in certain situations. We bring a new formulation of traffic pressure and traffic hysteresis. In that work, they showed that it's more desirable to have a macroscopic traffic model that can replicate the non-linear phenomenon and their characteristic properties. [11] showed that it's more desirable to have a macroscopic traffic model that can replicate the non-linear phenomenon and their characteristic properties. Hence a new traffic pressure from gas-kinetic will determine.

In this work, we are considering the road structure through the road inclination. It is incorporated in the anticipation term. This is because an incline on a multi-lane road is captured through the competition between Over Acceleration(OA) and Speed-Adaptation(SA) introduced by [10]. When a faster vehicle catches up with a slower one and cannot overtake, the driver decelerates within the synchronization space gap G adapting the speed to the speed of the preceding vehicle. This phenomenon is known as the SA. The vehicle SA lies in synchronized flow and is strongly related to the driving condition. This SA within the synchronization gap is associated with the 2D-region of steady states of synchronized flow. In contrary to the preceding case, a vehicle that moves in free flow on a multi-lane road approaches a slower moving preceding vehicle and has the possibility to overtake. He will first adapt his speed to the leader speed, change lane and accelerate. This phenomenon is known as OA.

The anticipation term is the way a driver adapt his speed to the traffic condition ahead. So we derive the anticipation term from the process of braking and acceleration illustrate first in [12]. In this work, we are bringing a stochastic source term in which the driver's decision is taken care of. The following model is more closed to the real traffic since it expressed the impact of driver's random behavior on the whole traffic. The particular driver's decision is figuring out

through a poisson process. A better understanding of this process can be found in [13]. Indeed a traffic flow is composed of random variables. Some of them depend on the driver's behavior, hence there exist as many behaviors as drivers on the road. However, some other variables can be classified as relating to their size.

2. PRELIMINARIES

2.1. Payne model. The first attempt using Gradient approach to derive a macroscopic traffic flow model traced back to Payne [15][14]:

$$\frac{\partial \rho}{\partial t} + \frac{\partial}{\partial x} Q(x, t) = 0$$

Where the flow rate $Q(x, t)$ is a function of the density $\rho(x, t)$ and the average velocity $V(x, t)$ or the velocity flow: $Q(x, t) = \rho(x, t)V(x, t)$.

Payne model is derived from the one of Newell [16]:

$$v_i(t + \tau) = v_o(d_i(t))$$

Where the speed of each vehicle is calibrate with a delay of τ to some optical speed v_o depending on the distance between the vehicle and his leader formulate as: $d_i = x_{i-1}(t) - x_i(t)$.

The corresponding macroscopic model was formulate as:

$$v_i(t + \tau) \approx V(x, t) + V\tau \frac{\partial V(x, t)}{\partial x} + \tau \frac{\partial V(x, t)}{\partial t}$$

Then he define the equilibrium velocity through:

$$V_e = v_o\left(\frac{1}{\rho}\right) \text{ or } V_e\left(\frac{1}{d_i}\right) = v_o(di) \text{ Where:}$$

$$\frac{1}{d_i(t)} \approx \rho(x, t) + \frac{1}{2\rho} \frac{\partial \rho(x, t)}{\partial x}$$

Then a first Taylor approximation of the previous equation give us:

$$v_o(d_i(t)) \approx V_e(\rho(x, t)) + \frac{dV_e(\rho)}{d\rho} \frac{\partial \rho(x, t)}{\partial x}$$

We end up with the final Payne model:

$$\frac{\partial V}{\partial t} + V \frac{\partial V}{\partial x} = \frac{1}{\tau} [V_e(\rho) - \frac{D(\rho)}{\rho} \frac{\partial \rho}{\partial x} - V(x, t)]$$

2.2. Properties of Payne model. In Payne's final model, the density-dependent diffusion $D(\rho)$ is:

$$D(\rho) = -\frac{dV_e(\rho)}{d\rho} = \frac{1}{2} \left| \frac{dV_e(\rho)}{d\rho} \right| \geq 0$$

The transport term $V \partial V / \partial x$ stands for the velocity motion profile. The anticipation term $-\frac{D(\rho)}{\rho}$ describes the reaction of drivers to the traffic situation in front of them. The relaxation term $[V_e(\rho) - V] / \Delta t$ describes the driver adaptation to the average velocity $V(x, t)$ to the density-dependent equilibrium velocity with a delay τ .

One weakness of the gradient expansion approach is that its validity implicitly requires small gradients. However, it is well-known that many microscopic and macroscopic traffic equations give rise to emergent traffic jams, which are related with steep gradients. That calls for the consideration of higher-order terms and leads to macroscopic traffic equations that are not anymore simple and well tractable (even numerically).

3. EXTENDED MODEL

The extended model is different from the preceding in the way the traffic pressure and anticipation are formulated. The road structure, the heterogeneous feature and the driver's behavior are better to represent.

3.1. The multi-valued anticipation term. The anticipation term is the way a driver adapt his speed to the traffic condition ahead. So we derive the anticipation term from the process of braking and acceleration. To adequately describe the braking and acceleration of cars and trucks on the multi-lane road, we derive the macroscopic traffic flow model for cars from the kinetic model of multi-lane traffic flow which uses distribution function. In the remaining of this paper, we consider a highway with 3lanes denoted by α such that $X_\alpha = 0, 1, 2, \dots, N$ and $X_\alpha = 3$ denoted the outer lane.

In this paper, we will only focus on the Gain and Loss due to braking and acceleration in [12]. We will also notice that the anticipation term is based on the one developed in [17] but differ with the inclusion of multi-lane aspect and road inclination:

$$(1) \quad \partial_t f_\alpha + v \partial_x f_\alpha = \tilde{C}_\alpha^+(f_1^2, \dots, f_N^2, f_1, \dots, f_N)$$

where:

$$\begin{aligned} \tilde{C}_\alpha^+(f_1^2, \dots, f_N^2, f_1, \dots, f_N) &= (G_B^+ - L_B^+)(f_{\alpha-1}, f_\alpha^2, f_{\alpha+1}) + (G_A^+ - L_A^+)(f_\alpha^2) \\ &+ [G_L^+(f_{\alpha-1}, f_\alpha^2) - L_R^+(f_{\alpha-1}, f_\alpha^2, f_{\alpha+1})] + [G_R^+(f_\alpha, f_{\alpha+1}^2, f_{\alpha+2}) - L_L^+(f_\alpha^2, f_{\alpha+1})] \end{aligned}$$

The gain and loss terms due to braking ie G_B^+, L_B^+ are given by:

(2)

$$\begin{aligned} &G_B^+(f_{\alpha-1}, f_\alpha, f_{\alpha+1}) \\ &= \iint_{\hat{v} > \hat{v}_+} P_B(\hat{v}, \hat{v}_+, f_{\alpha-1}(x + H_B(v)), f_{\alpha+1}(x)) |\hat{v} - \hat{v}_+| \sigma_B(v, \hat{v}_+) f_\alpha^2(x, \hat{v}, H_B(\hat{v}), v_+) d\hat{v} d\hat{v}_+ \end{aligned}$$

(3)

$$L_B^+(f_{\alpha-1}, f_\alpha, f_{\alpha+1}) = \int_{\hat{v} > \hat{v}_+} P_B(\hat{v}, \hat{v}_+, f_{\alpha-1}(x + H_B(v)), f_{\alpha+1}(x)) |\hat{v} - \hat{v}_+| f_\alpha^2(x, \hat{v}, h_B(\hat{v}), \hat{v}_+) d\hat{v}_+$$

The gain and loss term due to acceleration ie G_A^+, L_A^+ are given by:

(4)

$$G_A^+(f_\alpha) = \iint_{\hat{v} < \hat{v}_+} |\hat{v} - \hat{v}_+| \sigma_A(v, \hat{v}_+) f_\alpha^2(x, \hat{v}, x + H_A(\hat{v}, \hat{v}_+)) d\hat{v} d\hat{v}_+$$

(5)

$$L_A^+(f_\alpha) = \int_{v < \hat{v}_+} |v - \hat{v}_+| f_\alpha^2(x, v, x + H_A(v), \hat{v}_+) d\hat{v}_+$$

Where:

(6)

$$f_\alpha^2(x, \hat{v}, H_B(\hat{v}), \hat{v}_+) \sim q_B(H_B(\hat{v}); \hat{v}, f_\alpha(x, \hat{v})) F_\alpha(\hat{v}_+; H_B(\hat{v}), \hat{v}, x) f_\alpha(x, \hat{v})$$

Next we determine the closure relation of the distribution function $f_\alpha(x, v, t)$, as follow:

(7)

$$f_\alpha(x, v, t) = \rho_\alpha F_\alpha(x, v, t) = \rho_\alpha \delta u_\alpha(v)$$

where $\delta(v - u_\alpha(x, t)) = \delta u_\alpha(v)$ is the Dirac delta function and equation 7 is when all the vehicle have the same average velocity u_α at instantaneous time t .

We replace $f_\alpha^2(x, \hat{v}, H_B(\hat{v}), \hat{v}_+)$ in 2 and 3 by its approximation in 6, subtract the two preceding and integrate over $[0, w]$ to get:

(8)

$$\begin{aligned} \int_0^w v^k (G_B - L_B)(f_{\alpha-1}, f_\alpha, f_{\alpha+1}) dv &= P_B(u_\alpha, u_\alpha^+, \rho_{\alpha-1}^+, \rho_{\alpha+1}) |u_\alpha - u_\alpha^+| q_B(H_B(u_\alpha); u_\alpha, \rho_\alpha) \\ &\rho_\alpha \int_0^{V_{max}} v^k \sigma_B(v, \hat{v}) dv - P_B(u_\alpha, u_\alpha^+, \rho_{\alpha-1}^+, \rho_{\alpha+1}) |u_\alpha - u_\alpha^+| q_B(H_B(u_\alpha); u_\alpha, \rho_\alpha) \rho_\alpha u^k \end{aligned}$$

Then

$$(9) \quad \int_0^w v^k (G_B - L_B)(f) dv = P_B(u_\alpha, u_\alpha^+, \rho_{\alpha-1}^+, \rho_{\alpha+1}) |u_\alpha - u_\alpha^+| q_B(H_B(u_\alpha); u_\alpha, \rho_\alpha) [\rho_\alpha \int_0^{V_{max}} v^k \sigma_B(v, \hat{v}) dv - u^k]$$

using the following approximation, from [18]:

$$\sigma_B(v, u) \simeq \frac{\chi_{[\beta u, u]}(v)}{u(1-\beta)}$$

Where $\sigma_B(v, u)$ is a probability distribution denoting the imperfect adaptation of the faster vehicle with speed u_α to the speed u_α^+ of the leader and x is the road cross section where the probability of interactions occurring is high. We obtain:

$$(10) \quad \int_0^w v^k (G_B - L_B)(f) dv \simeq P_B(u_\alpha, u_\alpha^+, \rho_{\alpha-1}^+, \rho_{\alpha+1}) |u_\alpha - u_\alpha^+| q_B(H_B(u_\alpha); u_\alpha, \rho_\alpha) * \rho_\alpha \left[\frac{1}{u(1-\beta)} \int_{\beta u}^u v^k dv - u^k \right]$$

Considering that $u_\alpha^+(x) = u_\alpha(x + H_B)$ a braking occurs if $u_\alpha > u_\alpha^+$, $|u_\alpha - u_\alpha^+| = -(u_\alpha - u_\alpha^+)$

We obtain:

$$(11) \quad \int_0^w v^k (G_B - L_B)(f) dv \simeq -P_B(u_\alpha, u_\alpha^+, \rho_{\alpha-1}^+, \rho_{\alpha+1}) (u_\alpha^+ - u_\alpha) q_B(H_B(u_\alpha); u_\alpha, \rho_\alpha) * \rho_\alpha \left[\frac{u_\alpha^{k+1} - \beta u_\alpha^{k+1}}{(k+1)(u_\alpha - \beta u_\alpha)} - u_\alpha^k \right]$$

Equation 11 will vanish for $k = 0$ but not for $k = 1$. We have define below $u_\alpha^+(x) = u_\alpha(x + H_B)$ thus $u_\alpha^+(x) = u_\alpha(x) + H_B u_\alpha'(x)$. For the ease of writing H_B is approximate here by h and $u_\alpha'(x) = \partial_x u_\alpha$ leading to $(u_\alpha^+ - u_\alpha) \simeq h \partial_x u_\alpha$. We obtain at the end:

$$(12) \quad \int_0^w v^k (G_B - L_B)(f_{\alpha-1}, f_\alpha, f_{\alpha+1}) dv = P_B(u_\alpha, u_\alpha^+, \rho_{\alpha-1}, \rho_{\alpha+1}) \rho_\alpha q_B(h_B, \rho_\alpha) \rho_\alpha \frac{1-\beta}{2} u_\alpha \partial_x u_\alpha$$

With the same process we derived the balance equation from equation 4 and 5 to obtain:

$$(13) \quad \int_0^w v^k (G_A - L_A) f_\alpha dv = \rho_\alpha q_A(H_A(u_\alpha), \rho_\alpha) \left[\frac{\gamma-1}{2} \right] u_\alpha \partial_x u_\alpha$$

The function $q_X = (H_X(u_\alpha, \rho_\alpha))$ denotes the distribution of leading vehicles at distance h for a vehicle with velocity v under the assumption that the velocities of the vehicles are distributed according to the distribution function ρ_α [18]. Thus the distribution is some increasing function which is derived from the speed adaptation term in section 1.3. Moreover we use a suitable ansatz:

$$q_B(H(u_\alpha), \rho_\alpha) = q_A(H(u_\alpha), \rho_\alpha) = \frac{db(\rho_\alpha)}{d\rho_\alpha}$$

Such that

$$(14) \quad b(\rho_\alpha) = -\ln(1 - \rho_\alpha)$$

we obtain:

$$\int_0^w v^k C^+(f) dv \approx \begin{cases} \rho_\alpha \frac{db(\rho_\alpha)}{d\rho_\alpha} \varphi_B(u_\alpha, u_\alpha^+, \rho_{\alpha-1}, \rho_{\alpha+1}) u_\alpha \partial_x(u_\alpha), & \partial_x u_\alpha < 0 \\ \rho_\alpha \frac{db(\rho_\alpha)}{d\rho_\alpha} \varphi_A(u_\alpha) u_\alpha \partial_x(u_\alpha), & \partial_x u_\alpha > 0 \end{cases}$$

where $\varphi_B(u_\alpha, u_\alpha^+, \rho_{\alpha-1}, \rho_{\alpha+1}) = P_B(u_\alpha, u_\alpha^+, \rho_{\alpha-1}, \rho_{\alpha+1}) \frac{1-\beta}{2} u_\alpha$ and $\varphi_A(u_\alpha) = \frac{\alpha-1}{2} u_\alpha$

The impact of road inclination can be introduced through the parameters φ_B and φ_A . We will introduce the parameter θ such that if there is no inclination ($\theta = 0$), we have the value C and if $\theta \neq 0$, we have $D(v_m) > C$. Thus $a(\rho_\alpha, \theta)$ is the anticipation term describes as:

$$(15) \quad a(\rho_\alpha, \theta) = ce^{-v_m(\rho_\alpha, \theta)} \frac{\rho_\alpha}{1-\rho_\alpha}$$

The anticipation is a decreasing function depending on the road inclination θ and density ρ_α . More explicitly, the more the road inclination, the more the density and the anticipation term decrease as shown in figure 1

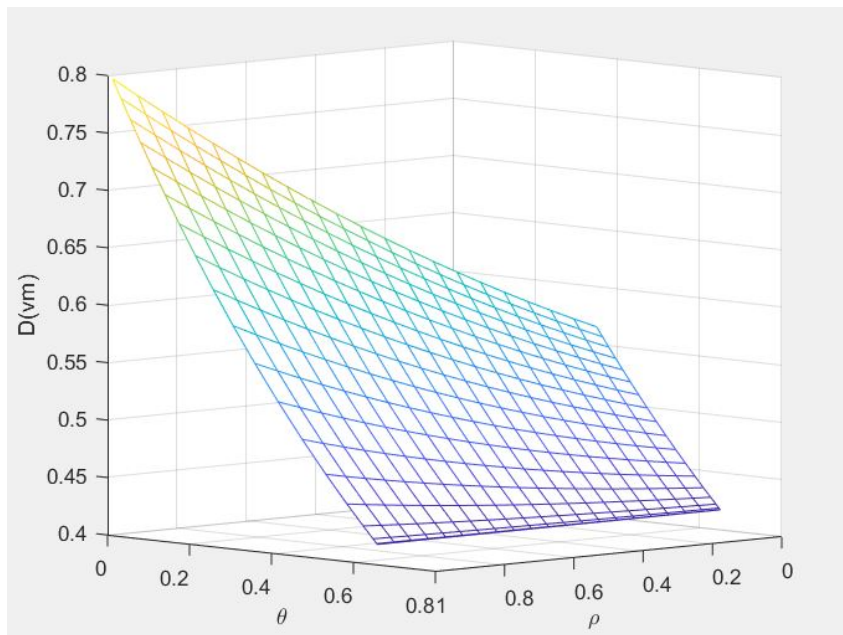


FIGURE 1. Anticipation curve due to road inclination θ and velocity of moving bottleneck

3.2. Heterogeneity of the traffic. Within a congested road section, a driver attempts to fill the space gap available by moving forward or changing lane. The driver's decision is modeled through a binomial function depending on whether the driver will move forward or change lane to a surrounding one, denoted ε_i . Furthermore, the area covered by a single vehicle on lane α , namely A_i^α is an integral function defined by:

$$A_i^\alpha = \int_0^{\beta_i} l_i dx \implies A_i^\alpha = l_i \beta_i^\alpha$$

where l is the vehicle width and β_i^α is the vehicle i length.

It yields to the following equation:

$$(16) \quad AO = \frac{1}{WTL} \sum_{\alpha=1}^m \sum_{i=1}^n t_i^\alpha A_i^\alpha \varepsilon_i$$

Where:

A_i : The road section on lane α occupied by vehicle i of class u during time t_i in m^2 will be defined later.

$t_{i,u}^\alpha$: The time during which a single section on a lane α is covered by vehicle i of class u .

T : The total observation.

L : The whole road stretch.

In real conditions it has been observed that drivers don't respect lane when there are some small width vehicle. so we will first use a multi-lane model numbered α with $\alpha = 1, 2, 3$. ε_i is defined as the i 'th driver's decision. The set of drivers is a set of random variables. So ε_i is a probabilistic decision determined from the stationary renewal process. To a better understanding of this process, we refer to [13]. Indeed when a driver is willing to change lane for one of the adjacent lanes, he will consider the density of the adjacent lane. If at time $t = t_0$ the space gap between him and his follower after an interaction is acceptable meaning his velocity after an interaction is sufficiently large, he will initiate the lane change otherwise he will wait and try again a time $t = t_0$. These operations are assimilated to the renewal process and for modeling, we will use the Poisson process to approximate this drivers decision function.

The Poisson process is a random counting process of points used in queuing theory to model random events. Using the renewal Poisson process we can take its pdf as our ϵ_i :

$$(17) \quad \epsilon_i = e^{-\rho_i C_o}$$

Thus the explicit equation of AO becomes:

$$(18) \quad AO = \frac{1}{WTL} \sum_{\alpha=1}^m \sum_{i=1}^n t_i^\alpha l_i \beta_i^\alpha e^{-\rho_n C_o}$$

3.3. Traffic pressure. We use the idea of [19] with our new Area Occupancy developed in the previous section. We derive our traffic pressure from a gas-kinetic parameter to which we apply the momentum method to get the macroscopic parameter. That is:

$$\int_0^{+\infty} \text{gas - kinetic} \rightarrow \text{macroscopic}$$

Instead of using the classical density, we will use A.O for specific lane: Let $s(|x' - x|) = s(x' - x) = s(x - x')$ a smooth function such that his normalization is $\int_{-\infty}^{+\infty} dx' s(x - x') = 1$ and we define the local density:

$$(19) \quad \rho(x, t) = \int_{-\infty}^{+\infty} dx' s(x - x') \frac{1}{TL} \sum_{\alpha} \sum_i^n t_i^\alpha A_{i,u}^\alpha \epsilon_n$$

We differentiate the local density with respect to time and applied the chain-rule:

$$(20) \quad \frac{\partial \rho(x, t)}{\partial t} = \frac{1}{TL} \int_{-\infty}^{+\infty} dx' \sum_i^n (-\frac{dx_i}{dt}) [\frac{\partial}{\partial x'} \sum_{\alpha} t_i^\alpha A_{i,u}^\alpha \epsilon_n] s(x - x')$$

We reformulate the parameters and applied the partial integration to the R.H.S of the previous result:

$$(21) \quad \int_{-\infty}^{+\infty} dx' [\partial_{x'} u(x')] v(x') = [u(x)v(x)]_{-\infty}^{+\infty} - \int_{-\infty}^{+\infty} u(x') [\partial_{x'} v(x')] dx'$$

In the previous equation $[u(x)v(x)]$ vanishes at the boundary, thus:

$$(22) \quad \frac{\partial \rho(x, t)}{\partial t} = -\frac{1}{TL} \frac{\partial}{\partial t} \int_{-\infty}^{+\infty} \sum_i^m v_i \sum_{\alpha} \sum_i^n t_i^\alpha A_{i,u}^\alpha \epsilon_n s(x - x') dx'$$

We use the symmetry of the smoothing function to obtain:

$$(23) \quad \frac{\partial}{\partial t} \rho(x, t) = -\frac{1}{TL} \frac{\partial}{\partial t} \int_0^{+\infty} \sum_i^m v_i \sum_{\alpha} \sum_i^n t_i^\alpha A_{i,u}^\alpha \epsilon_n s(x - x') dx'$$

$$(24) \quad \frac{\partial}{\partial t} \rho(x, t) = -\frac{1}{TL} \frac{\partial}{\partial t} [\rho(x, t) V(x, t)]$$

We derive the velocity variance from the derivative with respect to time:

$$(25) \quad [\rho(x, t)V(x, t)] = \sum_{\alpha}^m \sum_i^n v_i \frac{1}{TL} t_i^{\alpha} A_{i,u}^{\alpha} \epsilon_n$$

To get:

$$(26) \quad \frac{\partial}{\partial t} [\rho(x, t)V(x, t)] = \sum_{\alpha}^m \sum_i^n \frac{1}{TL} \frac{dv_i(t)}{dt} t_i^{\alpha} A_{i,u}^{\alpha} \epsilon_n + \sum_{\alpha}^m \sum_i^n \frac{1}{TL} v_i(t) \frac{dt_i^{\alpha}}{dt} A_{i,u}^{\alpha} \epsilon_n + \sum_{\alpha}^m \sum_i^n \frac{1}{TL} v_i(t) t_i^{\alpha} \frac{dA_{i,u}^{\alpha}}{dx_i} \frac{dx_i}{dt} \epsilon_n$$

$$(27) \quad \frac{\partial}{\partial t} [\rho(x, t)V(x, t)] = \sum_{\alpha}^m \sum_i^n \frac{1}{TL} a_i(t) t_i^{\alpha} A_{i,u}^{\alpha} \epsilon_n + \sum_{\alpha}^m \sum_i^n \frac{1}{TL} v_i(t) A_{i,u}^{\alpha} \epsilon_n + \sum_{\alpha}^m \sum_i^n \frac{1}{TL} [v_i(t)]^2 (t_i^{\alpha}) \frac{\partial A_{i,u}^{\alpha}}{\partial t} \epsilon_n$$

Thus the velocity variance takes the form:

$$\theta(x, t) = \frac{\int_{-\infty}^{+\infty} dx' \sum_{i=1}^m [v_i(t) - V(x, t)]^2 \delta(x' - x_i(t)) s(x - x')}{\int_{-\infty}^{+\infty} dx' \sum_{i=1}^m \delta(x' - x_i(t)) s(x - x')}$$

$$\theta(x, t) = \frac{\sum_{i=1}^m [v_i(t) - V(x, t)]^2 s(x - x')}{\sum_{i=1}^m s(x - x')}$$

$$\theta(x, t) = \frac{\sum_{i=1}^m [\delta v_i(t)]^2 s(x - x')}{\rho(x, t)}$$

At the end, we obtain the traffic pressure as:

$$(28) \quad P(x, t) = \frac{1}{WTL} \sum_{\alpha=1}^m \sum_{i=1}^n t_i^{\alpha} l_i \beta_i^{\alpha} e^{-\rho_n C_o} \theta(x, t) + \frac{v^o - v_e(\rho)}{2\tau}$$

Thus

$$(29) \quad P(x, t) = AO \cdot \theta(x, t) + \frac{v^o - v_e(\rho)}{2\tau}$$

Scatter properties of the second part of the fundamental diagram illustrated in [20] can be explained in the context of the new formulation of our traffic pressure as the heterogeneity of traffic. Indeed the simulation of equation 29 yields to some particles taking random direction over time as illustrate by figure 2 as predicted in [21].

Conversely, when we are trying to reduce the range value of vehicle size and drivers decision randomness we obtain a smooth increasing traffic pressure yielding to an ideal traffic like the one on figure 3

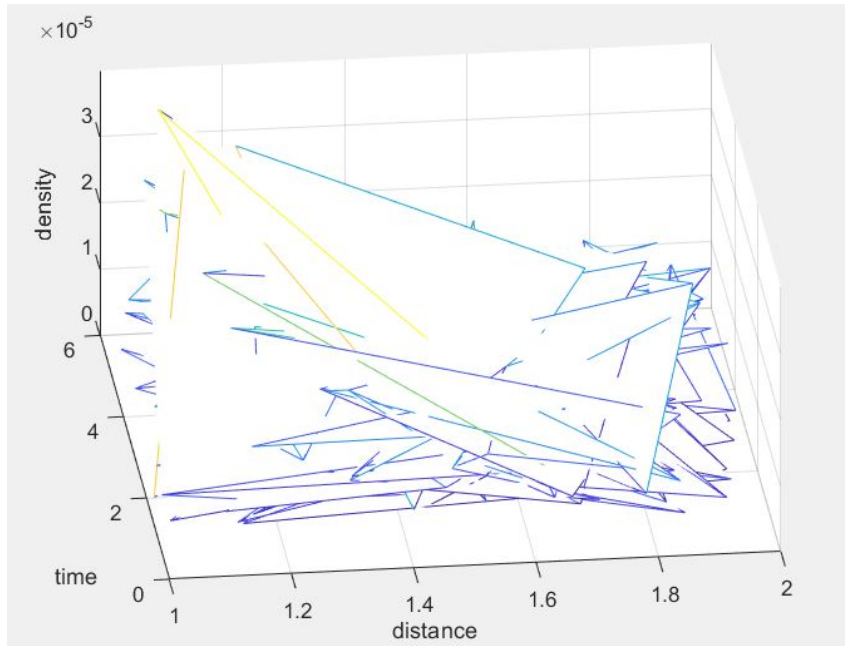


FIGURE 2. Stochastics traffic pressure

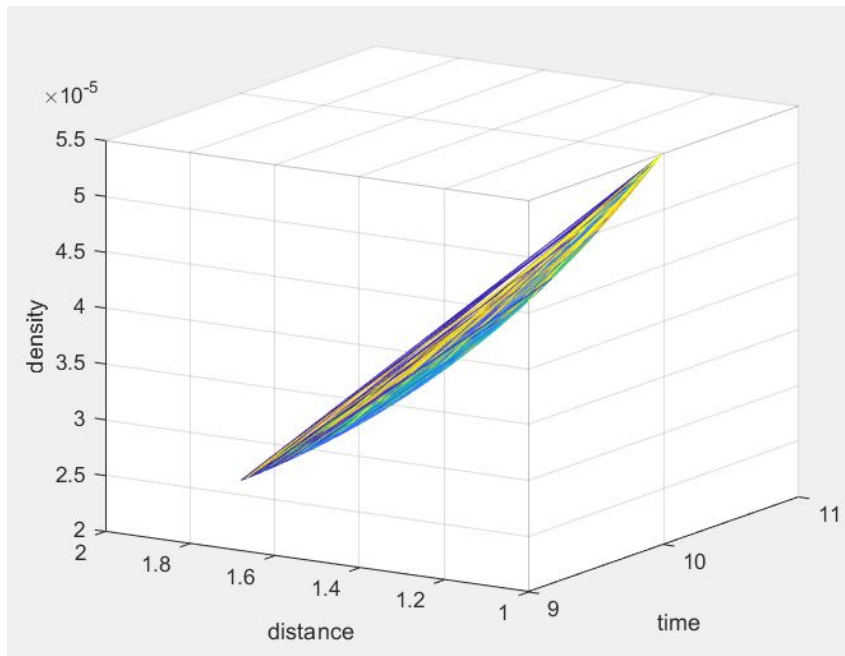


FIGURE 3. homogeneous traffic pressure

3.4. Hysteresis of the traffic. In this section, we will improve the fundamental diagram based on the scattered properties. Analyzing the one-minute empirical flow-density relationship of freeway M25 in England:

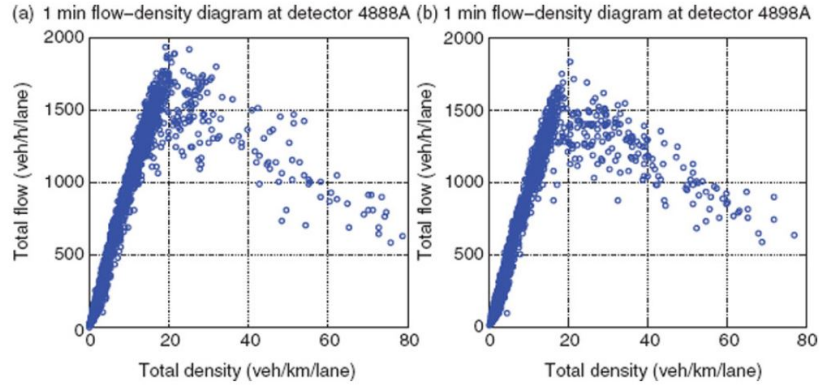


FIGURE 4. One-minute empirical flow-density relationships of freeway M25 in England

The graph show that the first part of the curve is parabolic and the second part which constitute scattered point will be modeled with the Brownian motion:

$$(30) \quad Q(\rho) = \begin{cases} v_{\max}\rho - \frac{v_{\max}-v_{crit}}{\rho_{crit}}\rho^2, & \text{if } \rho < \rho_{crit} \\ q(\rho), & \text{if } \rho > \rho_{crit} \end{cases}$$

We construct $q(\rho)$ with the Bachelier-Kolmogorov method. We consider a set of finite vehicle in which each driver has a particular decision to make, depending on the vehicle around. So we have some Gaussian random variables. At different times $t_0 = 0 < t_1 < \dots < t_n, t_j \in I$ and all the borel sets $A_1, \dots, A_n \in \mathbb{B}$ the finite dimensional distributions. Hence $P_{t_1}, \dots, P_{t_n}(A_1 \times \dots \times A_n) = \mathbb{P}(B_{t_1} \in A_1, \dots, B_{t_n} \in A_n)$ are mean-zero normal with covariance matrix $C = (t_j \wedge t_k)_{j,k=1, \dots, n}$

Theorem Cf [22] A one-dimensional Brownian motion is a Gaussian process $(B_t)_{t \geq 0}$. For $t_0 := 0 < t_1 < \dots < t_n, n \geq 1$, the vector $\Gamma := (B_{t_1}, \dots, B_{t_n})^T$ is a Gaussian random variable with a strictly positive definite, symmetric covariance matrix $C = (t_j \wedge t_k)_{j,k=1, \dots, n}$ and mean vector $m = 0 \in \mathbb{R}^n$:

$$(31) \quad \mathbb{E}e^{i\langle \xi, \Gamma \rangle} = e^{-\frac{1}{2}\langle \xi, C\xi \rangle}$$

Moreover, the probability distribution of Γ is given by:

$$(32) \quad \mathbb{P}(\Gamma) = \frac{1}{(2\pi)^{n/2} \sqrt{\prod_{j=1}^n (t_j - t_{j-1})}} \int \exp\left(-\frac{1}{2} \sum_{j=1}^n \frac{(x_j - x_{j-1})^2}{(t_j - t_{j-1})}\right) dx$$

From the previous theorem, the hysteresis can be formulate as:

$$(33) \quad P_{t_1, \dots, t_2}(A_1 \times \dots \times A_n) = \frac{1}{(2\pi)^{n/2} \sqrt{\prod_{j=1}^n (t_j - t_{j-1})}} \int \exp(-\frac{1}{2} \sum_{j=1}^n \frac{(x_j - x_{j-1})^2}{t_j - t_{j-1}}) dx$$

3.5. The new model. The R.H.S of our model is determined from the one developed in [17]. We will not expose the whole process but for a better understanding, we refer to that work.

In the original microscopic model equation containing the density ρ and his inverse τ , we will approximate the following parameters:

$$\tau \sim t \text{ and } \partial_x u \sim \frac{v_{i+1} - v_i}{H}$$

We remain with:

$$(34) \quad \begin{aligned} \partial_T t - \partial_X u &= 0 \\ \partial_T u - a(\frac{1}{\tau})u &= 0 \end{aligned}$$

Considering the first equation in the system 34, a variable separation leads to:

$$(35) \quad \partial_t \tau (\partial_T t) + \partial_x \tau (\partial_T x) - \partial_x u (\partial_X x) - \partial_t u (\partial_X t) = 0$$

Reducing the equation and multiplying through by $-\rho^2$, we obtained:

$$(36) \quad \partial_t \rho + u \partial_x \rho + \rho \partial_x u = 0$$

The same process used for the second equation of the system 34 leads to:

$$(37) \quad [\rho \partial_t u + u \partial_t \rho] + [2\rho u \partial_x u + u^2 \partial_x \rho] - a(\rho) \partial_x u = 0$$

Combining equations 36 and 37:

$$(38) \quad \begin{aligned} \partial_t \rho + \partial_x(\rho u) &= 0 \\ \partial_t(\rho u) + \partial_x(\rho u^2) - a(\rho, \theta) \partial_x u &= 0 \end{aligned}$$

Combining the system 38 with the source term constitute of the traffic pressure 29 and the hysteresis 33 we obtain:

$$(39) \quad \begin{aligned} \partial_t \rho + \partial_x(\rho u) &= 0 \\ \partial_t(\rho u) + \partial_x(\rho u^2) - a(\rho, \theta) \partial_x u &= AO \cdot \theta(x, t) + \frac{v^o - v_e(\rho)}{2\tau} + \frac{1}{(2\pi)^{n/2} \sqrt{\prod_{j=1}^n (t_j - t_{j-1})}} \int \exp(-\frac{1}{2} \sum_{j=1}^n \frac{(x_j - x_{j-1})^2}{t_j - t_{j-1}}) dx \end{aligned}$$

which can be recast in its quasi-linear form:

$$\begin{aligned}
 & \partial_t \rho + \partial_x(\rho u) = 0 \\
 (40) \quad & \partial_t(u) + \partial_x\left(u^2 - \frac{a(\rho, \theta)}{\rho}u\right) = AO \cdot \theta(x, t) + \frac{v^o - v_e(\rho)}{2\tau} + \\
 & \frac{1}{(2\pi)^{n/2} \sqrt{\prod_{j=1}^n (t_j - t_{j-1})}} \int \exp\left(-\frac{1}{2} \sum_{j=1}^n \frac{(x_j - x_{j-1})^2}{t_j - t_{j-1}}\right) dx
 \end{aligned}$$

4. NUMERICAL ANALYSIS

The feature of traffic flow model is given by the eigenvalue and eigenvector of the RHS of the system. Thus we will first focus on the RHS of the system. The system 40 can be expressed in the following form:

$$(41) \quad \partial_t U + \partial_x F(u) = S(u)$$

Where:

$$U = \begin{bmatrix} \rho \\ u \end{bmatrix}$$

and

$$F(u) = \begin{bmatrix} \rho u \\ u - \frac{a(\rho)}{\rho} \end{bmatrix}$$

4.1. Riemann Variables. The quasi-linear form of the model give us:

$$(42) \quad \begin{cases} \frac{\partial U}{\partial t} + j(u) \frac{\partial U}{\partial x} = S(u) \\ U(x, 0) = \begin{cases} U_L & \text{if } x < 0 \\ U_R & \text{if } x > 0 \end{cases} \end{cases}$$

Where $j(u) = \frac{\partial F(U)}{\partial U}$ and

$$j(u) = \begin{bmatrix} u & \rho \\ 0 & u - \frac{a(\rho)}{\rho} \end{bmatrix}$$

$$\det|j(u) - \lambda I| = 0 \implies \lambda_1 = u - \frac{a(\rho)}{\rho} \text{ and } \lambda_2 = u$$

For $\lambda_1 = u - \frac{a(\rho)}{\rho}$,

$$E_1 = \begin{bmatrix} 1 \\ -\frac{a(\rho)}{\rho^2} \end{bmatrix}$$

For $\lambda_2 = u$,

$$E_2 = \begin{bmatrix} 1 \\ 0 \end{bmatrix}$$

$\lambda_1 < \lambda_2$ implies that the macroscopic traffic flow model is hyperbolic. Moreover, the anisotropic character of the model is preserved because the traffic information travels faster than the traffic.

We determine the nature of the wave through the dot product $\nabla\lambda_i R^i$.

$$\begin{aligned} \begin{pmatrix} \partial_\rho \lambda_1 \\ \partial_u \lambda_1 \end{pmatrix} \cdot \begin{pmatrix} 1 \\ -\frac{a(\rho)}{\rho^2} \end{pmatrix} &= \begin{pmatrix} -\partial_\rho \left(\frac{a(\rho)}{\rho^2}\right) \\ 1 \end{pmatrix} \cdot \begin{pmatrix} 1 \\ -\frac{a(\rho)}{\rho^2} \end{pmatrix} \\ \begin{pmatrix} \partial_\rho \lambda_1 \\ \partial_u \lambda_1 \end{pmatrix} \cdot \begin{pmatrix} 1 \\ -\frac{a(\rho)}{\rho^2} \end{pmatrix} &= -\partial_\rho \left(\frac{a(\rho)}{\rho^2}\right) - \frac{a(\rho)}{\rho^2} \neq 0 \end{aligned}$$

and

$$\begin{pmatrix} \partial_\rho \lambda_2 \\ \partial_u \lambda_2 \end{pmatrix} \cdot \begin{pmatrix} 1 \\ 0 \end{pmatrix} = 0$$

Thus The 1st characteristic associate to λ_1 is genuinely non-linear and the 2nd characteristic related to λ_2 field is linearly degenerate. Therefore we end up with a hyperbolic system where the 1st characteristic is shock wave and the 2nd is a contact discontinuity. Let r denotes the so-called Riemann variable and δU a variation of U (either $\delta U/\delta t$ or $\delta U/\delta x$), we define $\delta r = M^{-1}\delta U$ and $\delta U = M\delta r$. Thus we obtain $M\frac{\partial r}{\partial t} = \frac{\partial U}{\partial t}$ and $M\frac{\partial r}{\partial x} = \frac{\partial U}{\partial x}$. The define matrix of the eigenvector ε is:

$$M = \begin{pmatrix} 1 & 1 \\ -\frac{a(\rho)}{\rho^2} & 0 \end{pmatrix}$$

with

$$M^{-1} = \begin{pmatrix} 0 & -\frac{\rho^2}{a(\rho)} \\ 1 & \frac{\rho^2}{a(\rho)} \end{pmatrix}$$

We use these matrices in 42 to get:

$$(43) \quad M^{-1}M\frac{\partial r}{\partial t} + M^{-1}j(u)M\frac{\partial r}{\partial x} = \tilde{S}$$

Thus Equation 43 becomes:

$$(44) \quad \frac{\partial r}{\partial t} + V\frac{\partial r}{\partial x} = \tilde{S}$$

where $\tilde{S} = \varepsilon^{-1}S$ and

$$V = \begin{pmatrix} \lambda_1 & 0 \\ 0 & \lambda_2 \end{pmatrix} \implies V = \begin{pmatrix} u - \frac{a(\rho)}{\rho} & 0 \\ 0 & u \end{pmatrix}$$

If we consider the definition of the Riemann (or characteristic) variables, we obtain:

$$(45) \quad \delta r_1 = \delta u - \frac{a(\rho)}{\rho} \delta \rho$$

and

$$(46) \quad \delta r_2 = \delta u$$

A simple integration give us:

$$(47) \quad r_1 = u - a(\rho) \ln(\rho) \quad \text{and} \quad r_2 = u$$

4.2. Stability of the model. The aim of this section is to prove that the model prevents vehicles from moving backwards. For this sake we will use the HLLE scheme. The outline of the scheme can be found in many literature but we refer to [24]. The HLLE scheme is a numerical scheme for high order model based on the the approximated Riemann solution and Godunov scheme.

The approximation of the traffic variable at each cell i to the mean value of the exact solution U of system 41:

$$(48) \quad U_i(k) = \frac{1}{\Delta x} \int_{-\infty}^{+\infty} U(x,t) dx$$

And solving the Riemann problem at cell interfaces couple with the theory of divergence gives:

$$(49) \quad \frac{d}{dt} \int_{x_{i-1/2}}^{x_{i+1/2}} U(x,t) dx + \frac{F(U(x_{i+1/2},t)) - F(U(x_{i-1/2},t))}{\Delta x} = 0$$

Where $F(U(x_i + 1/2, t))$ is the flux at each time step and each cell interface. The solution of the Riemann problem is given by:

$$(50) \quad \tilde{U}_{i+1/2} \left(\frac{x - x_{i+1/2}}{t} \right) = \begin{cases} U_i & \text{if } x - x_{i+1/2} < x_{i+1/2}^l t \\ U_{i+1/2} & \text{if } x_{i+1/2}^l t < x - x_{i+1/2} < x_{i+1/2}^r t \\ U_{i+1} & \text{if } x - x_{i+1/2} > x_{i+1/2}^r t \end{cases}$$

Where: $\chi^r(i+1/2, k) = \max(\chi^{\max}(i+1/2, k), \chi^{\max}(i+1, k))$ and $\chi^l(i+1/2, k) = \min(\chi^{\min}(i+1/2, k), \chi^{\min}(i, k))$ are respectively the maximum and the minimum of the eigenvalue of the system.

However the average intermediate state of equation 50 must satisfies the following conservation law:

$$(51) \quad \int_{-\Delta x/2}^{+\Delta x/2} \tilde{U}_{i+1/2}(x/t) dx = \int_{-\Delta x/2}^{+\Delta x/2} \tilde{U}(x/t) dx$$

Hence:

$$(52) \quad U(i+1/2, k) = \frac{\chi^r(i+1/2, k)U(i+1, k) - \chi^l(i+1/2, k)U(i, k) - \frac{F(i+1, k) - F(i, k)}{\chi^r(i+1/2, k) - \chi^l(i+1/2, k)}}{\chi^r(i+1/2, k) - \chi^l(i+1/2, k)}$$

And the fluxes are determine by:

$$(53) \quad F(i+1/2, k) = \frac{\chi^+(i+1/2, k)F(i, k) - \chi^-(i+1/2, k)F(i+1, k) - \frac{\chi^+(i+1/2, k)\chi^-(i+1/2, k)}{\chi^+(i+1/2, k) - \chi^-(i+1/2, k)}(U(i+1/2, k) - U(i, k))}{\chi^+(i+1/2, k) - \chi^-(i+1/2, k)}$$

Where $\chi^+(i+1/2, k) = \max(\chi^r(i+1/2, k), 0)$ and $\chi^-(i+1/2, k) = \min(\chi^l(i+1/2, k), 0)$ are respectively largest and smallest wave speed.

Applying the above method to the system 41 we obtained:

$$(54) \quad u(i, k+1) = u(i, k) - \frac{\Delta t}{\Delta x}(\rho(i+1/2, k) - \rho(i-1/2, k))$$

$$(55) \quad \rho(i, k+1) = \rho(i, k) - \frac{\Delta t}{\Delta x}[(u - \frac{a(\rho)}{\rho})(i+1/2, k) - (u - \frac{a(\rho)}{\rho})(i-1/2, k)] + Hyst(i, k) + TP(i, k)$$

Where $Hyst(i, k)$ is the hysteresis and $TP(i, k)$ is the Traffic pressure.

Analyzing of the scheme in two extreme cases: upstream congested/downstream free flow and upstream free flow/downstream congested.

- Upstream free flow/downstream congested:

In this case $U(i, k) \rightarrow 0$ at $t = k\Delta t$:

$$(56) \quad \frac{\partial u}{\partial t} = \frac{1}{\Delta x}(\rho(i+1/2, k) - \rho(i-1/2, k))$$

Where:

$$(57) \quad \rho(i+1/2, k) = \frac{-\chi^-(i+1/2, k)U(i+1, k)}{\chi^+(i+1/2, k)-\chi^-(i+1/2, k)} [u - (u - \frac{a(\rho)}{\rho})] \geq 0$$

$$(58) \quad \rho(i-1/2, k) = \frac{\chi^+(i+1/2, k)\rho(i-1, k)}{\chi^+(i+1/2, k)-\chi^-(i+1/2, k)} + \frac{-\chi^+(i-1/2, k)\chi^-(i-1, k)U(i-1, k)}{\chi^+(i+1/2, k)-\chi^-(i+1/2, k)} \geq 0$$

We replace the different parameters by theirs values in the Riemann problem resolution to end up with:

$$(59) \quad \rho(i+1/2, k) = \frac{(u-a(\rho)/\rho)U(i+1, k)}{a(\rho)/\rho} \geq 0$$

Thus $\partial U/\partial t \geq 0 \implies$ at every time $t \geq t_o$. Since we are in free flow at cell i , $\partial \rho/\partial t$ has the same sign as $\partial u/\partial t$. Hence $\partial \rho/\partial t \geq 0 \implies \rho(x, t) \geq 0$ at every time $t > t_o$

- Downstream free flow/upstream congested:

For this case, in cell i $\rho(i, k) \rightarrow \rho_{max}$ at $t_o = \Delta t$

$$(60) \quad \frac{\partial(\rho)(i, k+1)}{\partial t} = \frac{1}{\Delta x} [(u - \frac{a(\rho)}{\rho})(i+1/2, k) - (u - \frac{a(\rho)}{\rho})(i-1/2, k)] + H_{yst}(i, k) + TP(i, k)$$

Where

$$(61) \quad (u - \frac{a(\rho)}{\rho})(i+1/2, k) = \frac{-\chi^-(i+1/2, k)U^2(i+1, k)}{\chi^+(i+1/2, k)-\chi^-(i+1/2, k)} [u^2(i+1, k) + (\frac{a(\rho)}{\rho})^2(i+1/2, k) - \chi^+(i+1/2, k)\frac{a(\rho)}{\rho}(i+1, k)]$$

$$(62) \quad (u - \frac{a(\rho)}{\rho})(i-1/2, k) = \frac{\chi^+(i-1/2, k)}{\chi^+(i+1/2, k)-\chi^-(i-1/2, k)} (u - \frac{a(\rho)}{\rho})(i-1, k) + \frac{-\chi^+(i-1/2, k)\chi^-(i-1/2, k)}{\chi^+(i+1/2, k)-\chi^-(i-1/2, k)} (\rho)(i-1, k) \geq 0$$

We use of equation to get:

$$(63) \quad (u - \frac{a(\rho)}{\rho})(i+1/2, k) = \frac{-u(i+1/2, k)U^2(i+1, k)}{\frac{a(\rho)}{\rho}(i+1/2, k)} [u^2(i+1, k) + (\frac{a(\rho)}{\rho})^2(i+1/2, k) - u(i+1/2, k)\frac{a(\rho)}{\rho}(i+1, k)] \leq 0$$

Thus $\partial \rho(i, k+1)/\partial t \geq 0 \implies \rho(x, t) \geq 0$ at every time $t > t_o$. Since traffic in cell i is congested $\partial \rho/\partial t$ has the opposite sign, meaning $\partial u/\partial t \leq 0 \implies \rho(x, t) < \rho_{max}$ at every time $t > t_o$

In conclusion, it was found that the vehicles do not move backward and the traffic is anisotropic(from downstream to upstream). Moreover it has been proven in [23] that the HLLE scheme is stable and accurate over time.

4.3. Propagation of disturbance. We decoupled including the eigenvalues to get:

$$(64) \quad \begin{aligned} \frac{\partial r_1}{\partial t} + \lambda_1 \frac{\partial r_1}{\partial x} &= \tilde{S}_1 \\ \frac{\partial r_2}{\partial t} + \lambda_2 \frac{\partial r_2}{\partial x} &= \tilde{S}_2 \end{aligned}$$

Regarding the system, the Riemann variable propagates along the corresponding characteristic curve with speed λ_1, λ_2 . The corresponding characteristics curves are $C^+ : dx = \lambda_2 dt$ and $C^- : dx = \lambda_1 dt$. Let $P(x, t)$ be a point in the space, we determine the speed and the density from r_2, r_1 transported with speed λ_2, λ_1 along the curve C^-, C^+ :

$$(65) \quad \begin{aligned} (r_1)_p &= u = (r_1)_{p+} \\ (r_2)_p &= u - a(\rho) \ln(\rho) = (r_1)_{p-} \end{aligned}$$

The maximal wave speed corresponding to λ_2 travel faster than the traffic itself. Thus propagates downstream leading to the formation of the jam

5. SIMULATION

The data used for the simulation have been collected on *Autoroute du nord, axe Adjame-Yopougon*

Model parameters	
Max speed(km/h)	108
critical speed(km/h)	86.4
jam density(km/h)	0.14veh/m
critical density(km/h)	0.019veh/m
Maximum vehicle length(m)	30
Simulation duration(s)	1800
Cfl number	0.999
Highway characteristics	
Length(m)	7600
Width	3.3
Inclination	0.3

We will apply the above parameters to the Godunov method to confirm what has been found numerically. The simulation will give us the flow, density and speed. For the ease of simulation the heterogeneity of the traffic is fixed and extended to fundamental diagram whereby the vehicles are taking a value between the shortest vehicle and the longest one.

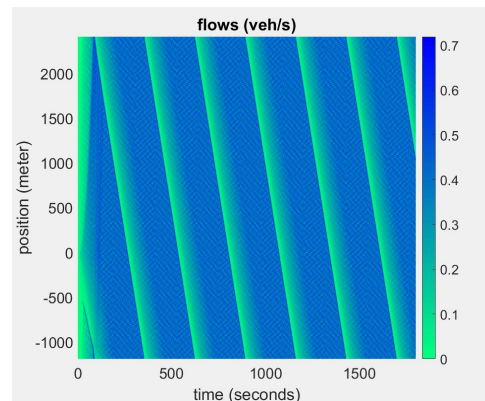


FIGURE 5. Vehicle flow

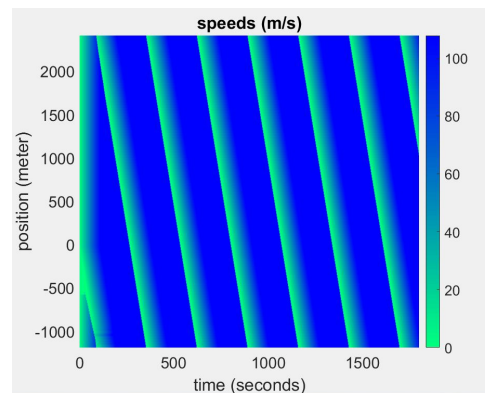


FIGURE 6. vehicle-speed

The figures 5 & 6 shows the evolution of traffic on the highway. We brought a model describing Kerner's features of traffic name $F \rightarrow S \rightarrow J$. Then the stop and go waves are also well represented. The figure 7 show up one of the principle in traffic flow which states that the traffic jam is always an inverse function of the flow.

6. RESULT AND DISCUSSION

In this paper, we have shown the road inclination decrease drastically the speed of trucks. Since the velocity of the flow is more relate to the speed of the trucks all the traffic slow down

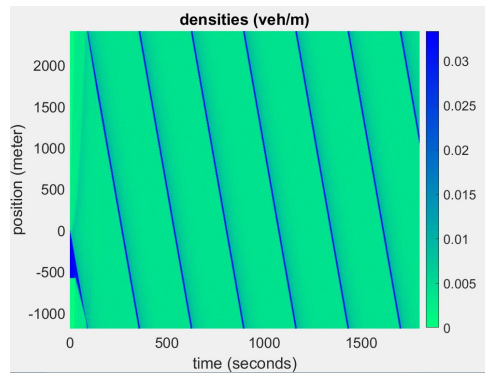


FIGURE 7. jam-density

depending on the average of trucks on the highway so the anticipation term decrease. The stochasticity of the traffic heterogeneity is an improvement of the former one. The traffic pressure has shown that the drivers decision depend on the size of the vehicle around. The more the traffic becomes homogeneous the more the speed of the speed of the and the drivers decision become less random. The new model yields to the three-phase theory traffic as it is an extension of Payne model. Among the usual traffic properties, the new model is hyperbolic, stable and we observe the shock and rarefaction. The rarefaction describe the discontinuity on the highway leading to stop and go waves in real condition

But the lack of microscopic data for this particular traffic prevented us to well calibrate the source term accurately. Also the correlation between the heterogeneity and the drivers decision must be deeply investigate to prescribe better recommendation on the road management. Moreover he calibration can give us better recommendation about the percentage of trucks which must be allowed to avoid huge jam through the traffic pressure.

ACKNOWLEDGMENTS

I would like to express my heartfelt appreciation to Pan African University, Institute for Basic Sciences, Technology and Innovation(Kenya) financial support and also I am grateful to Dr Mark Kimathi for his help on the development of this paper.

CONFLICT OF INTERESTS

The author(s) declare that there is no conflict of interests.

REFERENCES

- [1] G.H. Peng, X.H. Cai, B.F. Cao, C.Q. Liu, Non-lane-based lattice hydrodynamic model of traffic flow considering the lateral effects of the lane width, *Phys. Lett. A*, 375 (30–31) (2011), 2823-2827.
- [2] C. Mallikarjuna, K.R. Rao, Area occupancy characteristics of heterogeneous traffic, *Transportmetrica*, 2 (3) (2006), 223-236.
- [3] P. Athol, *The Interdependence of Certain Operational Characteristics Within a Moving Traffic Stream*, Expressway Surveillance Project, 1963.
- [4] W.F. Phillips, A new continuum traffic model obtained from kinetic theory. 1978 IEEE Conference on Decision and Control including the 17th Symposium on Adaptive Processes. IEEE, 1979.
- [5] R. Fuller, Towards a general theory of driver behaviour, *Accident Anal. Prevent.* 37 (3) (2005), 461-472.
- [6] R. Fuller, J.A. Santos, Psychology and the highway engineer. In R. Fuller and J.A. Santos (Eds.), *Human factors for highway engineers*. Pergamon, Oxford, 2002.
- [7] J.A. Laval, L. Ludovic, A mechanism to describe the formation and propagation of stop-and-go waves in congested freeway traffic. *Phil. Trans. R. Soc. A, Math. Phys. Eng. Sci.* 368 (1928) (2010), 4519-4541.
- [8] G.F. Newell, Theories of instability in dense highway traffic, *J. Oper. Res. So. Japan*, 5 (1) (1962), 9-54.
- [9] C.F. Daganzo, Requiem for second-order fluid approximations of traffic flow, *Transport. Res. Part B., Methodol.* 29 (4) (1995), 277-286.
- [10] B.S. Kerner, L.K. Sergey, Phase transitions in traffic flow on multilane roads, *Phys. Rev. E*, 80 (5) (2009), 056101.
- [11] B.S. Kerner, S. Boris, K. Peter, Cluster effect in initially homogeneous traffic flow, *Phys. Rev. E*, 48 (4) (1993), R2335.
- [12] A. Klar, R. Wegener, A hierarchy of models for multilane vehicular traffic I: Modeling, *SIAM J. Appl. Math.* 59 (3) (1998), 983–1001.
- [13] S. Karlin, H.M. Taylor, *A first course in stochastic processes*, 2nd Edition, Academic Press, 2014.
- [14] H.J. Payne, A critical review of a macroscopic freeway model, *Research Directions in Computer Control of Urban Traffic Systems*, ASCE, 1979, 251-256.
- [15] H.J. Payne, *Models of freeway traffic and control*, *Mathematical Models of Public Systems*, 1971.
- [16] G.F. Newell, Nonlinear effects in the dynamics of car following, *Oper. Res.* 9 (2) (1961), 209-229.
- [17] M.E. Kimathi, *Mathematical Models for 3-Phase Traffic Flow Theory*, Diss. 2012.
- [18] A. Klar, R. Wegener, Kinetic derivation of macroscopic anticipation models for vehicular traffic, *SIAM J. Appl. Math.* 60 (5) (2000), 1749-1766.
- [19] D. Helbing, Derivation of non-local macroscopic traffic equations and consistent traffic pressures from microscopic car-following models. *Eur. Phys. J. B*, 69 (4) (2009), 539-548.

- [20] S.C. Calvert, H. Taale, S.P. Hoogendoorn, Quantification of motorway capacity variation: influence of day type specific variation and capacity drop. *J. Adv. Transport.* 50 (4) (2016), 570-588.
- [21] F. Wageningen-Kessels, H. Lint, K. Vuik, S. Hoogendoorn, Genealogy of traffic flow models. *Eur. J. Transport. Logist.* 4 (4) (2015), 445-473.
- [22] R.L. Schilling, L. Partzsch, *Brownian motion: an introduction to stochastic processes.* Walter de Gruyter GmbH & Co KG. 2014.
- [23] B. Einfeldt, C.D. Munz, P.L. Roe, B. Sjögreen, On Godunov-type methods near low densities. *J. Comput. Phys.* 92 (2) (1991), 273-295.
- [24] D. Ngoduy, *Macroscopic discontinuity modelling for multiclass multilane traffic flow operations.* TRAIL thesis series, Ngoduy D, Delft University Press, 2006.